IMPLICATIONS OF CLIMATE CHANGE DUE TO THE ENHANCED GREENHOUSE EFFECT ON FLOODS AND DROUGHTS IN AUSTRALIA

P. H. WHETTON, A. M. FOWLER, M. R. HAYLOCK, and A. B. PITTOCK
Climate Impact Group, CSIRO Division of Atmospheric Research, P.M.B. No. 1, Mordialloc 3195, Australia

Abstract. Potential impacts of climate change on heavy rainfall events and flooding in the Australian region are explored using the results of a general circulation model (GCM) run in an equilibrium enhanced greenhouse experiment. In the doubled CO_2 simulation, the model simulates an increase in the frequency of high-rainfall events and a decrease in the frequency of low-rainfall events. This result applies over most of Australia, is statistically more significant than simulated changes in total rainfall, and is supported by theoretical considerations. We show that this result implies decreased return periods for heavy rainfall events. The further implication is that flooding could increase, although we discuss here the many difficulties associated with assessing in quantitative terms the significance of the modelling results for the real world.

The second part of the paper assesses the implications of climate change for drought occurrence in Australia. This is undertaken using an off-line soil water balance model driven by observed time series of rainfall and potential evaporation to determine the sensitivity of the soil water regime to changes in rainfall and temperature, and hence potential evaporation. Potential impacts are assessed at nine sites, representing a range of climate regimes and possible climate futures, by linking this sensitivity analysis with scenarios of regional climate change, derived from analysis of enhanced greenhouse experiment results from five GCMs. Results indicate that significant drying may be limited to the south of Australia. However, because the direction of change in terms of the soil water regime is uncertain at all sites and for all seasons, there is no basis for statements about how drought potential may change.

1. Introduction

The possibility of changes in the frequency or intensity of floods and droughts in response to an enhanced greenhouse effect has received little attention in the literature on climate change. However one only needs to consider the present impact of floods and droughts in the Australian environment to realise that any change in their occurrance could be one of the most important regional impacts of global warmng. The damage cost in Australia from flooding events is particularly high when urban areas are involved. For example, as a result of the flood that affected the Sydney area in August 1986, damage worth approximately $A100 million occurred, and six lives were lost (Lynch, 1987). Rural flooding results in significant crop and stock losses and increased erosion. Overall, Joy (1991) has estimated that the annual cost of flooding to Australia is $A380 million. Recurrent drought is also

Climatic Change **25:** 289–317, 1993.

a hazard over much of Australia under the present climate, with a prime cause being rainfall fluctuations due to the El Niño – Southern Oscillation (ENSO). These droughts impose a significant cost on the Australian community, through declines in rural production, incomes and employment, increases in soil erosion, and the risk of forest fires. For example, during the severe drought of 1982/83, there was a decline in the value of rural exports of $500 million with a significant flow-on to the economy in general (Campbell *et al.*, 1983).

In the first part of this paper (Sections 3–5) we consider the impact of climate change on heavy rainfall events, through an analysis of changes to simulated daily rainfall for Australia under enhanced greenhouse conditions using the CSIRO 9-level model (CSIRO9). Simulated changes in total rainfall, mean rainfall intensity, and number of raindays are examined. To examine possible implications of the results for changes in extreme rainfall events and flooding, we use return period analysis. The study can be viewed as an extension, for Australia, of the analysis of Gordon *et al.* (1992) which used an earlier four-level version of the CSIRO model (CSIRO4). In an enhanced greenhouse experiment, Gordon *et al.* identified, globally, an increase in convective rainfall at the expense of non-convective rainfall, significant increases in the frequency of high rainfall events, and, in midlatitudes, a decrease in the number of raindays. They also showed a significant shortening of the return period of heavy rainfall events over Australia and elsewhere. Apart from the regional focus, the current study differs from Gordon *et al.* (1992) in two important respects. First, the GCM used is significantly improved in a number of ways over that used in the earlier study. The increase in the vertical resolution from four to nine levels is the most significant, particularly as this provides scope for more detailed representation of atmospheric precipitation processes. Second, the examination of rarely-occurring extreme events is facilitated by the availability of at least 28 years of data for each run of CSIRO9 compared to the ten years of CSIRO4 data used by Gordon *et al.* (1992).

In Section 6 of the paper, where the impact of climate change on drought is considered, a rather different approach is employed. Because of the much greater temporal scale of drought events as compared to flood events, there is much less need to examine changes in rainfall on a daily timescale (although changes in rainfall intensity and the frequency of rainy days may be of some significance). First order changes in drought potential are likely to arise from shifts in climatic means, and it is this effect that we examine here. Furthermore, an examination of changes in precipitation only is insufficient, because under enhanced greenhouse conditions changes in evaporation may be just as important. The impact on soil water must be examined. However, for a number of reasons (detailed in Section 6), GCM-simulated soil water is considered unreliable and potentially misleading in the context of assessing climate change impacts on drought. Potential drought impacts in the Australian region are therefore assessed using an 'off-line' soil water balance model. This is used to assess the sensitivity of the soil water regime at nine sites, representing a range of climate regimes and possible future climates. The model is

driven by observed daily time series of rainfall and potential evaporation, adjusted for a range of possible climate futures as suggested by GCM results. Apart from circumventing some of the inadequacies of GCM-simulated soil hydrology, use of an off-line model in this manner has two advantages. First, a range of site factors important in determining the nature of potential impacts can be accommodated, such as vegetation type and soil hydraulic characteristics. Second, repeated model runs allows assessment of potential impacts across a range of plausible future climates. We take advantage of this in the current study by using a set of regional climate change scenarios for 2030 (Appendix) based on the results of four other recent GCM enhanced greenhouse experiments as well as those of CSIRO9. To address the issue of drought we present results here on simulated changes in the return period of episodes of significantly reduced soil water.

Any study of climate change and its impacts at the regional scale is fraught with uncertainties. Although we do not believe that the problems are so great as to invalidate the work we present here, the caveats are numerous and significant and need to be clearly stated. They are discussed in the section that follows.

2. Caveats

GCM results, particularly for rainfall, can differ significantly from model to model at the regional scale (Houghton *et al.*, 1990). This means that, as far as possible, the results of a number of GCMs should be considered in any assessment of regional climate change. Thus the results we present here for changes in daily rainfall intensity are limited in that they are drawn from only one GCM. This problem is alleviated through reference, where possible, to relevant results from other GCMs. The problem does not affect our study of changes in soil water. The GCM data requirements for the drought study were much less and we were able to use results from a range of GCMs.

CSIRO9 and the other GCM experiments used in this study use a simple ocean representation which does not include the deep ocean or ocean currents. Also, the perturbed climate in these experiments is for equilibrium $2 \times CO_2$ conditions, not for the more realistic scenario of steadily increasing CO_2. However, the results from recent experiments with coupled-ocean atmosphere models that attempt to simulate the transient behaviour of future climate, indicate that major differences from the equilibrium results occur only in high latitude oceanic areas (Houghton *et al.*, 1992).

There are a number of difficulties which currently preclude quantitative estimation of how simulated changes in rainfall intensity may affect particular locations and catchments within any region. The coarse horizontal and vertical resolution of the CSIRO9 model, and other GCMs of the present generation, results in crude simulation of rainfall processes. Convective cells in the model can have a linear extent no smaller than a model grid square (around 500 km square), whereas in the real atmosphere their areal extent is typically orders of magnitude less than this.

Consequently the model cannot reproduce rainfall frequency distributions (and particularly the most intense rainfall daily totals) recorded at individual stations. This is even more the case in regions where local topography and small scale atmospheric circulation systems unable to be resolved in the model (such as tropical cyclones) are important in determining rainfall patterns. Furthermore, due to errors in rainfall rates in the control simulation of a model, the daily rainfall statistics derived from the control and doubled CO_2 simulations may not apply quantitatively even for large-area averages. In addition, the data sets available from CSIRO9 (and GCMs generally) are only of short duration (up to 30 years from CSIRO9), and for that reason alone GCMs may not capture rarely occurring, but significant, events. Due to these problems, but particularly that of spatial scale incompatibility, changes in model-generated daily rainfall totals, such as those examined here, are indicative only. They cannot be viewed as providing accurate quantitative guidance on how observed daily rainfall frequency distributions may change with global warming.

No consideration is given to possible changes in ENSO due to global warming. This caveat is particularly applicable to our analysis of drought. Observed year to year variability of rainfall in Australia is strongly influenced, especially in the north and east, by ENSO (Pittock, 1975; Nicholls and Woodcock, 1981; Pittock, 1984). ENSO is not simulated in CSIRO9 nor in any of the GCMs used in preparing the climate change scenarios used in Section 6. However, despite ENSO's importance in the Australian region, it accounts for at most only about one third of the total variance in seasonal rainfall in the areas most strongly affected (Pittock, 1984), so that studies that do not include ENSO variations still provide useful information. Little is known about the possible response, if any, of ENSO to the enhanced greenhouse effect, although ENSO-like features are simulated in the latest coupled ocean-atmosphere GCM experiments (e.g. Meehl *et al.*, 1993). Further development of coupled ocean-atmosphere GCMs is required before reliable simulations of ENSO and its response to global warming will be possible. However, it should be noted that current interannual variability in rainfall due to ENSO is included in our analysis here of drought, through the use of observed rainfall data (modified for climate change).

Due to these difficulties, the analysis to be undertaken in this paper cannot lead to quantitative predictions of how extreme rainfall events and drought may change over Australia as a result of global warming. However, it does have the scope to indicate what the direction of change may be and whether the impacts have the potential to be significant.

3. Rainfall Intensity: Physical Arguments and GCM Results

Theoretically, an increase in heavy rainfall events can be expected in response to global warming. Satellite observations and theory indicate that the amount of precipitable water in a vertical column over the oceans increases, non-linearly, with

increasing sea surface temperature (Stephens, 1990). Thus the amount of water vapour available for rainfall is greater for higher base temperatures typical of the tropics or a warmer climate due to enhanced greenhouse conditions. This increase would be expected to generally apply for Australian rainfall, which is usually due to moisture transported from over the oceans. Furthermore, the condensation of the available water vapour in the convective systems releases latent heat which further increases the strength of the convective activity (see further discussion in Gordon *et al.*, 1992).

A tendency for increased convective activity can be seen in the results obtained from enhanced greenhouse experiments with general circulation models (see Houghton *et al.*, 1990, p. 153). For example, Noda and Tokioka (1989), who examined changes in various rainfall types in an enhanced greenhouse experiment, found an increase in the frequency of intense convective rainfall and a decrease in less intense non-convective rainfall. Consistent results have also been obtained by Hansen *et al.* (1988) and Wetherald and Manabe (1988) in enhanced CO_2 experiments.

As a result of increased convection, changes in the frequency distribution of grid point daily rainfall totals would be expected in the models. Gordon *et al.* (1992) have shown, using data from many grid points, that CSIRO4 shows a general increase in the frequency of high-rainfall events, and, in midlatitudes, a decrease in the number of raindays. Similar results have emerged in a preliminary global analysis of the results of CSIRO9 (Pittock, in press) and with the high resolution UKMO GCM (J. Gregory, pers. comm.). Consistent with more heavy rainfall events, Mearns *et al.* (1990) found greater variability in daily rainfall over the United States in an enhanced greenhouse GCM experiment. However, similar studies of model results by Rind *et al.* (1989) and Wilson and Mitchell (1987) for the United States and Europe respectively did not obtain a clear change in rainfall intensity.

4. Changes in Rainfall Characteristics in the Australian Region Simulated by CSIRO9

The Model

The modelling results used here come from an enhanced greenhouse experiment conducted by I. Watterson and M. Dix which involved running CSIRO9 to equilibrium for 330 ppm of carbon dioxide (control simulation) and then again under conditions of double this concentration of carbon dioxide ($2 \times CO_2$). The atmospheric model was coupled to a simple mixed layer ocean, and a 'Q-flux' correction was applied (see Gordon *et al.*, 1992). The horizontal resolution of this R21 spectral model is approximately 3.2×5.6 degrees. The rainfall simulated by CSIRO9 can be grouped into two classes: large-scale rain due to saturation in one or more layers of the model atmosphere and rain due to convection involving over-

turning of at least two adjacent layers in the model atmosphere. The convection scheme used is a modified Arakawa moist-adjustment scheme which generates a mass flux (see Gordon *et al.*, 1992). For further details of CSIRO9 see McGregor *et al.* (1993), and for details of the similar experiment performed with CSIRO4, see Gordon *et al.* (1992).

For the control and $2 \times CO_2$ runs of the model there are 28–30 years of data available (depending on whether daily or monthly rainfall data are examined). All of the results presented here use at least twenty-eight years of data. Under doubled CO_2 conditions the model simulates a globally averaged increase in temperature of 4.8 °C and an increase in rainfall of 10%. Other GCM studies yield increases ranging from 1.7–5.3 °C and 3–15% respectively (see Houghton *et al.*, 1990, 1992).

The performance of CSIRO9 at simulating observed global climate is comparable with other current GCMs (McGregor *et al.*, 1993), and is, in general, improved over CSIRO4 (presented in Whetton and Pittock, 1991; and Gordon *et al.*, 1992). CSIRO9 also stood out as one of the best performing models in a recent intercomparison of how 16 GCMs simulated monsoon variability in India and Africa (WMO, 1992). Figure 1 compares zonally averaged precipitation for DJF and JJA as observed (Jaeger, 1976) and as simulated by CSIRO9 in the $1 \times CO_2$ run of the current experiment. Agreement is good, although it is poorest in the high latitudes of the southern hemisphere in DJF where rainfall is notably less than observed (but also where observed data may be significantly in error – see Houghton *et al.* (1990)). The performance is comparable to that of other recent GCMs (see figure 4.10 in Houghton *et al.* (1990)). Figure 2 shows annual zonal averages of simulated convective and non-convective precipitation. No direct comparison with observations is possible here, but the result is in qualitative agreement with the common observation that rainfall is predominantly convective in nature in the tropics, and stratiform (non-convective) in nature in high latitudes.

Greater confidence can be placed in a model which also simulates climate of the region of interest adequately. Maps showing DJF and JJA average daily rainfall rate for both the model and as observed are shown in Figure 3. The observed maps are based on station rainfall data for all available years of record obtained from the Australian Bureau of Meteorology. CSIRO9 simulates the main features of seasonal rainfall distribution in the Australian region. Northern and eastern Australia receives most rainfall in summer and the very strong annual cycle in rainfall in the monsoon-dominated far north of Australia is well simulated. The predominance of winter rainfall in southern, and particularly southwestern, Australia is also represented by the model. However, simulated rainfall gradients are not strong enough, with the result that inland areas are generally too wet and coastal areas too dry. This is most noticeable in winter, where inland rainfall totals are around twice the observed. To some extent this problem must be expected, because the coarse horizontal resolution of the model does not allow climatically important topography to be fully represented. The spatial distribution of rainfall over Australia is much

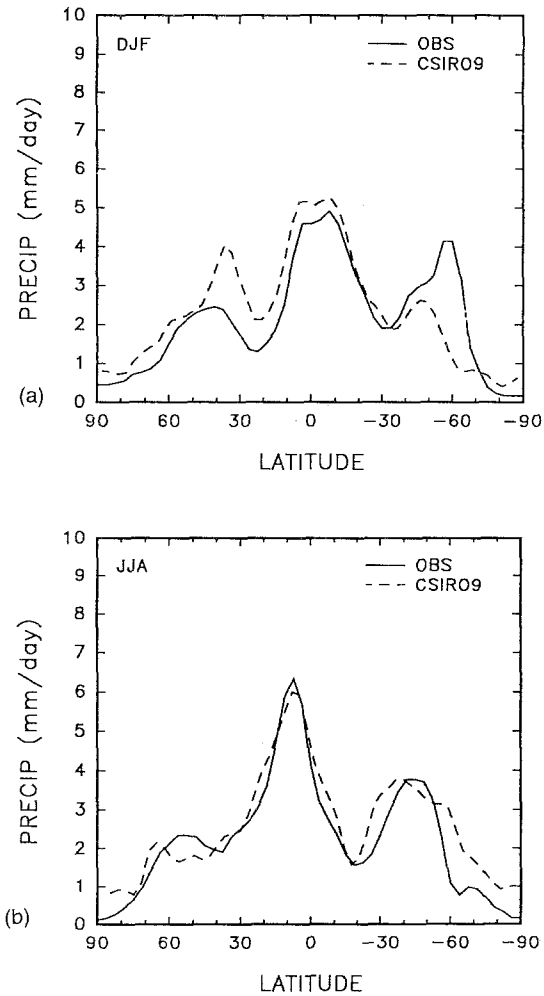

Fig. 1. (a) Summer (DJF); and (b) winter (JJA) zonally averaged precipitation: observed and CSIRO9 control simulation.

improved over that of CSIRO4, particularly in summer (see Whetton and Pittock, 1991), and is comparable to that achieved by other recent models (see Figure 4.11 in Houghton *et al.*, 1992). We have also examined CSIRO9 control simulation of surface temperature and mean sea level pressure along with those of four other recent GCMs. CSIRO9 and the other models reproduced the broadscale climatic features of the region (Whetton, 1993) unlike some earlier GCM simulations (Whetton and Pittock, 1991).

Due to the problem of scale incompatibility (discussed in Section 2), it is not clear how to interpret any comparison against observed climate of daily rainfall frequency distributions of the model, and such a comparison is not presented here.

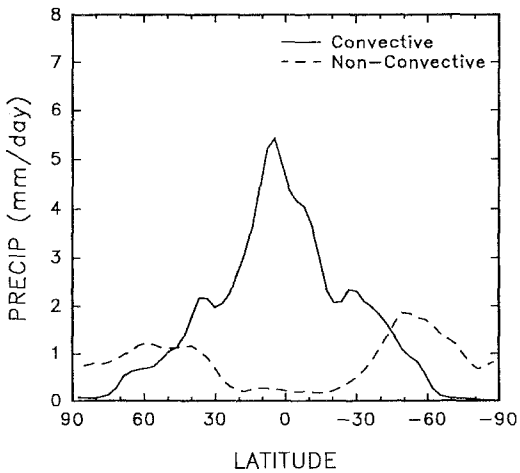

Fig. 2. Annual zonally averaged convective and non-convective precipitation simulated by CSIRO9 under control conditions.

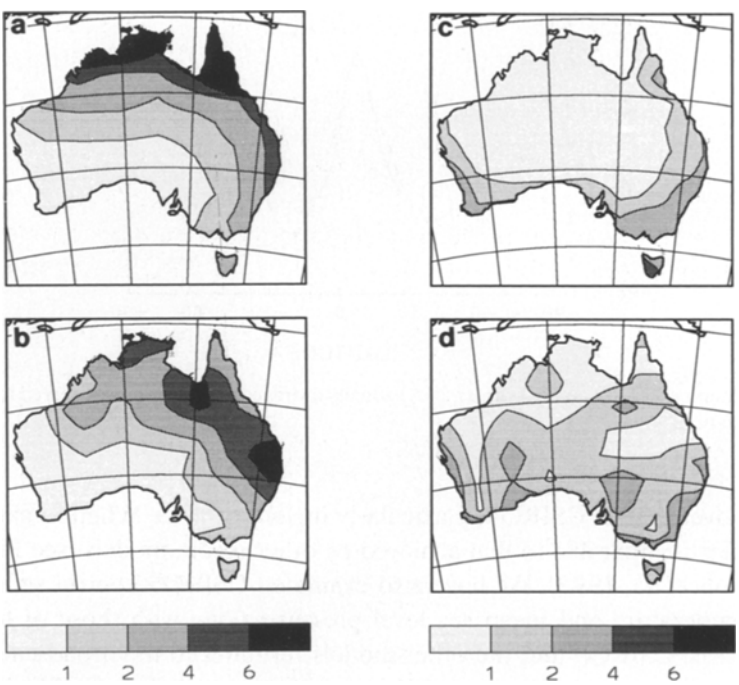

Fig. 3. Comparison of Australian region observed and CSIRO9-simulated seasonal precipitation: (a) DJF observed; (b) DJF simulated; (c) JJA observed; and (d) JJA simulated.

How best to relate model grid point daily rainfall to station rainfall is a difficult problem, and will be a subject of future research.

2× CO_2 Results

Change in annual rainfall in the doubled CO_2 simulation is shown in Figure 4a. Increases of up to 20% occur over most of the continent, but decreases occur in the region of the east coast. Statistical significance of the changes was assessed, on a grid point by grid point basis, using a simple Student's *t*-test of the difference of the means for control and doubled CO_2 of the annual averages of total rain. Increases significant at the 95% confidence level cover much of the continent, whereas significant rainfall decreases are apparent on the east coast. Changes in annual and seasonal total rainfall for the region, averaged by latitude, are shown in Figure 5. North of about 33° S, there is strong seasonality in the simulated rainfall change, with marked increases in summer and decreases in winter. This seasonal pattern of simulated rainfall change for the region is qualitatively similar to that obtained in other recent GCM experiments (see Appendix and Whetton, 1993).

A grid point by grid point *t*-test, such as used in Figure 4a will be satisfied over some of the domain simply due to chance. The likelihood of getting a significant region as large as that in Figure 4a by chance (field significance) can be calculated but allowance needs to be made for spatial inter-correlation in the data. This is achieved in the 'Pooled Permutation Procedure' (see Preisendorf and Barnett (1983) and Wigley and Santer (1990)), where the twenty-eight years of data from each of the control and doubled CO_2 simulations are pooled, and a reference distribution is created by analysing a large number of randomly selected pairs of twenty-eight years. Here one thousand random trials were used, and the number of *t*-test significant points in Figure 4a was found to be significant at greater than the 99.9% level.

Figure 6 shows the simulated change in total rainfall over the Australian region (as defined in Figure 4), broken down by type and averaged by latitude. In each latitude band there is increased convective rainfall in the doubled CO_2 experiment compared to the control. There is also a slight tendency for non-convective rain to decrease outside the tropics. The simulated change in rainfall under $2 \times CO_2$ conditions represents an increase in the proportion of total rainfall of the more intense convective type more characteristic of the tropics, and a decrease in the proportion of the less intense large scale (stratiform) rainfall type characteristic of the midlatitudes.

Figures 4b and 4c show changes over Australia in the annual average number of rain days, and rain per rainday (rainfall intensity). (A rainday is defined as a day with at least 0.2 mm of rainfall). Under enhanced greenhouse conditions, the number of raindays declines over much of eastern and southern Australia and increases elsewhere (Figure 4b). The decline is significant in the region of the east coast and over the southern ocean. Significant increases occur in the far north. The overall

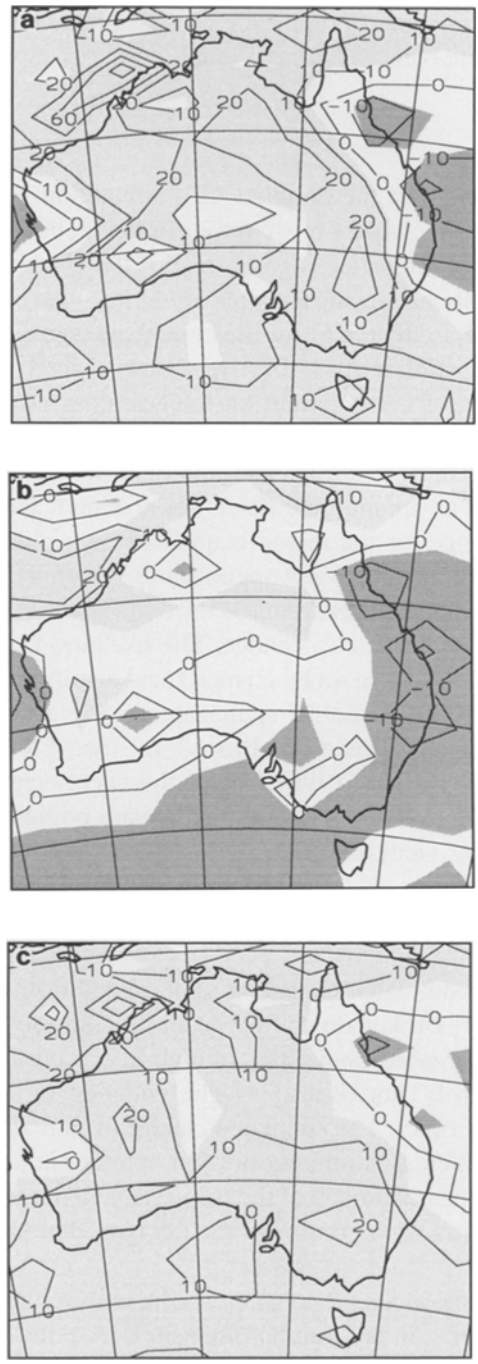

Fig. 4. Percentage change of average annual rainfall (a); number of raindays (b); and rain per rainday (c) in the doubled CO_2 model simulation relative to that in the control simulation. Light stippling represents areas of increase significant at the 95% level using a *t*-test. Heavy stippling represents significant decrease.

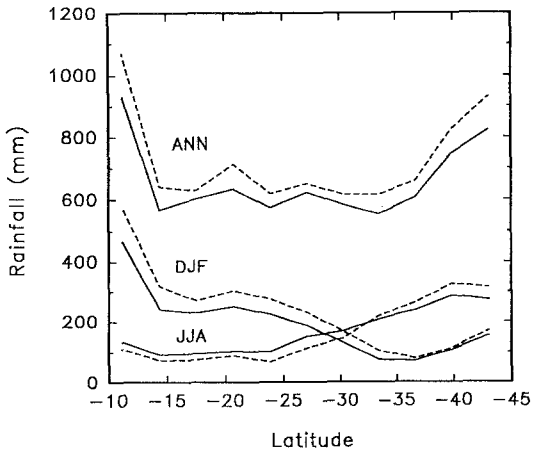

Fig. 5. Latitudinal averages of total rainfall, combined for all grid points at each latitude in the region depicted in Figure 4 for control simulation (full lines) and the doubled CO_2 simulation (dashed lines). Results are shown separately for summer (DJF), winter (JJA) and annual averages (ANN).

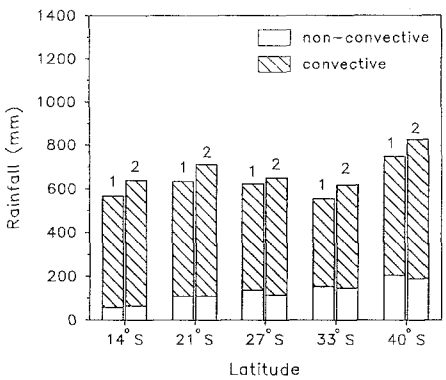

Fig. 6. Total average annual rainfall over the region shown in Figure 4 for the control (1) and doubled CO_2 (2) simulations, averaged by latitude and divided according to rainfall type.

pattern of change is field significant at the 99.9% level. Fewer raindays in the mid-latitudes may reflect the change in that zone in the relative contributions of large-scale and convective rainfall as indicated in Figure 6. A decline in the number of raindays suggests more frequent or longer dry spells between rainfalls.

Rain per rainday (Figure 4c) increases over almost the entire region, including some areas of total rainfall decrease. The area of significant change includes most of the region, is field significant at the 99.9% level, and is more extensive than the area of significant change for total rainfall (Figure 4a). Thus, for the Australian region, the model is more clearly indicating a change in rainfall intensity in response to the enhanced greenhouse effect than a change in total rainfall amount.

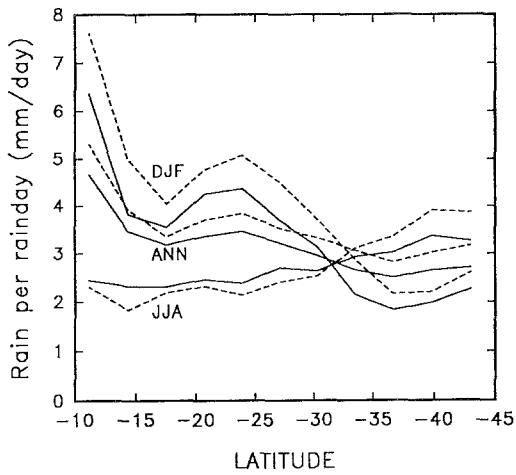

Fig. 7. Latitudinal averages of rain per rainday (rainfall intensity), combined for all grid points at each latitude in the region depicted in Figure 4 for control simulation (full lines) and the doubled CO_2 simulation (dashed lines). Results are shown separately for summer (DJF), winter (JJA) and annual averages (ANN).

Changes in annual and seasonal rain per rainday values, averaged by latitude, are shown in Figure 7. The increase in rainfall intensity is most marked in summer. In winter, where a decrease in total rainfall was simulated (see Figure 5), there is also a decrease in rainfall intensity, although a little less marked. Figure 7 also indicates that the model simulates greater rainfall intensity in low compared to higher, latitudes and in summer compared to winter. This is in qualitative agreement with observations.

The increases in rain per rainday are reflected in the frequency distribution of daily rainfall amounts. We calculated annual frequency distributions for $1 \times CO_2$ and $2 \times CO_2$ conditions, averaged over all Australian land points, and, for comparison, averaged over the full latitudinal bands at 40° N and 40° S. Frequencies were calculated in logarithmically spaced classes in order to provide a near normal distribution. Figure 8 shows the results in terms of percentage change between the $1 \times CO_2$ and $2 \times CO_2$ model simulations. For Australia, reductions in the lower classes are of the order 5%. In all three cases, there are decreases in the number of raindays in all rainfall classes up to and including 3.2–6.4 mm/day and increases in the two higher classes. Changes are more substantial for higher rainfall classes: over 10% increase for the 6.4–12.8 mm class and over 50% for the highest class.

These rainfall frequency change results are consistent with those of CSIRO4. Although in quantitative terms the results of the two models differ, both show the general pattern of significantly increased daily rainfall intensity along with marked increases in the frequency of simulated heavy rainfall events and decreases in the frequency of light rainfall events (see Gordon *et al.*, 1992; and Houghton *et al.*, 1992, pp. 119–120). Furthermore, similar analysis of southern hemisphere daily

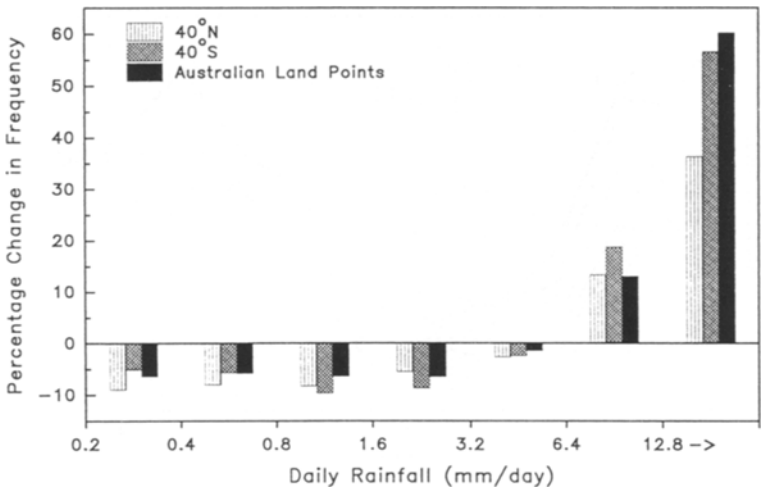

Fig. 8. Percentage change in the frequency of CSIRO9-simulated daily rainfall totals for various classes at latitudes 40° N and 40° S, and for 42 Australian land points. Results are for raindays (>0.2 mm) and are combined for all gridpoints.

rainfall frequency distributions in the high resolution UKMO equilibrium experiment (see Houghton *et al.*, 1990) shows a similar response (Hennessy *et al.*, 1993).

5. Changes in the Frequency of Extreme Rainfall Events: Implications for Flooding in Australia

A primary concern in flood-related planning is the frequency of occurrence of extreme events above some design threshold, typically expressed in terms of the return period of the event. To investigate the flooding implications of the changes in rainfall frequency discussed above, the daily rainfall results were re-analysed in terms of return periods. Daily rainfall amounts corresponding to seven selected return periods (3 and 6 months, 1, 2, 4, 7 and 14 years) were calculated at each model grid point for both the $1 \times CO_2$ and $2 \times CO_2$ simulations. Almost all grid-points show an increase in the daily rainfall amounts corresponding to each return period (at least 88% of grid-points over the 42 Australian land gridpoints for all seven return periods). Latitudinal averages of percentage increase in the size of events with a given return period are shown in Figure 9, across the region as defined in Figure 4. Increases range from 7% to 27%, and are somewhat higher for longer return periods. Notable latitudinal patterns are evident in Figure 9, including lower increases (ca. 10%) between 17° S and 28° S and an increasing trend from 28° S to 37° S.

A different perspective of the significance of the return period results is gained by examining the change in the frequency of threshold events. This is evident in

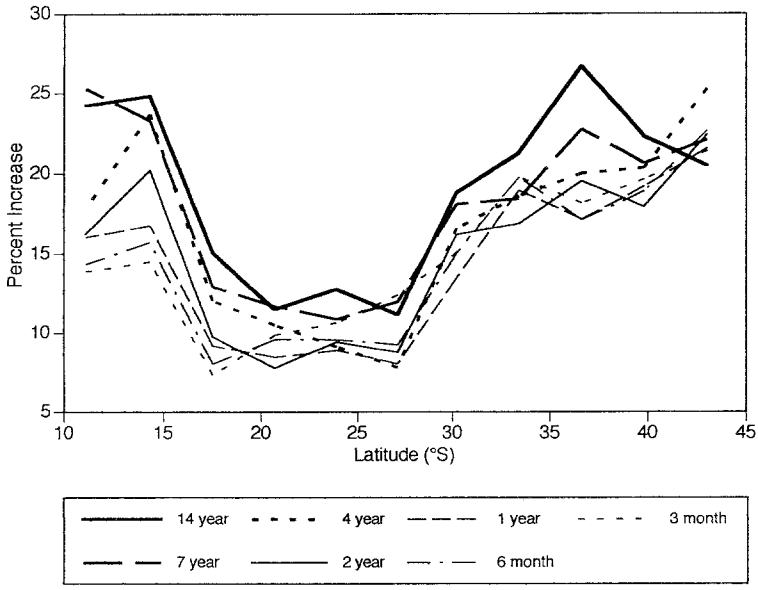

Fig. 9. Percentage change in the amount of rainfall corresponding to different return periods (14, 7, 4, 2, 1 years; 6, 3 months) under $2 \times CO_2$ relative to $1 \times CO_2$ conditions. Latitudinal averages are calculated for the region shown in Figure 4.

Figure 10, where daily rainfall corresponding to different return periods, and averaged over all 42 Australian land grid-points, is plotted against return period for both the $1 \times CO_2$ and $2 \times CO_2$ simulations. Two features of this graph are particularly noteworthy. First, the displacement of the $2 \times CO_2$ results above those for $1 \times CO_2$ conditions indicates a substantial increase in the frequency of daily events corresponding to each return period (calculated under current climate). Second, divergence of the two regression lines indicates an amplification of the effect as the return period lengthens. For example, whereas the one-year event in the control simulation occurs twice as frequently in the $2 \times CO_2$ simulation (becomes a 6-month event), the 10-year event becomes about a 3-year event. Seasonal analysis (not shown) indicated a reduction in return periods in each of the four seasons except winter, with the largest reduction in summer. These changes in frequency of return period events are comparable to those simulated for Australia by CSIRO4 (Gordon *et al.*, 1992).

We re-emphasise the caveats outlined in Section 2, particularly the mismatch in spatial scale between GCM-simulated gridpoint rainfall and rainfall events as they are observed in the real world. For these reasons, the results presented here should be viewed only as a qualitative guide as to how the occurrence of extreme rainfall events might change under enhanced greenhouse conditions. Our decision to present some results in these circumstances is in part a response to the fact that flood-related planning is not climate-neutral, but often carries an implicit assump-

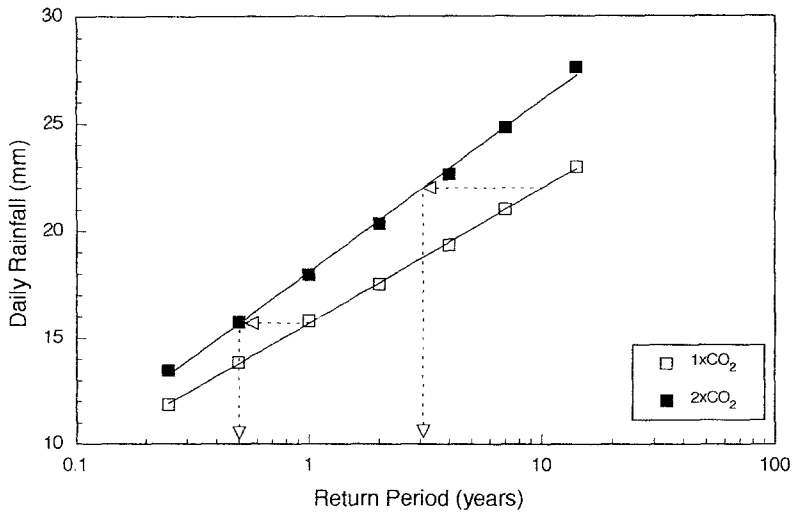

Fig. 10. Daily rainfall (mm) corresponding to different return periods, as simulated by CSIRO9 and averaged across all 42 land gridpoints in the Australian region. Least squares regression lines are shown. Arrows show the change in the return period of the one-year and ten-year events, as defined in the control simulation.

tion that the climate of the recent past is representative of the climate of the future. Since this is a probably incorrect projection of future climate, our view is that there is an onus on climate researchers to provide as much detail as possible on potential changes in the frequency of extreme rainfall events, but with the caveats strongly emphasised.

The return periods discussed here are relatively short, but are relevant to flood-related design. For example, Robinson (1987) noted that return periods as short as two years have been used as the basis for engineering design in Australia for road works, urban drainage, and minor bridges (rarely), while the 5-year event is frequently used for drainage and, in some cases, minor bridges and culverts, and even some minor dam spillways. Consequently, if these model results are indicative of the scale of potential impacts on extreme rainfall events due to climate change over the next half century (the time scale over which an effective doubling of CO_2 could be expected), there are significant flooding implications. The amplification of the changes as the return period lengthens suggests that the implications for longer return periods (more commonly used as design levels) may be serious.

Change in the frequency of design events has implications for the cost of future construction, since larger, more expensive, and intrusive structures would be required to cope with increased volumes of runoff. However, potentially far more serious are the implications for existing flood mitigation schemes and drainage systems. A doubling of the frequency of the design event by definition means a doubling of the frequency of system 'failure'. Assuming that the design event does in fact represent an acceptable level of risk, it follows that the indicated frequency

changes may result in an unacceptable new risk level, requiring costly remedial work.

An important example of this may be in dam spillway design. Due to an upward revision in probable maximum rainfall estimates for Australia (for reasons unrelated to the enhanced greenhouse effect), modifications to dams in New South Wales costing an estimated $A500 million in total are needed to achieve the intended risk level (Smith and Greenaway, 1987). Our results suggest a possible increase in probable maximum rainfall under enhanced greenhouse conditions. Thus, as climate changes, further, and perhaps more extensive, modifications could be required to achieve the desired risk level.

If more frequent and severe flooding were to occur, the social and economic costs of changing existing infrastructure to cope with this would be significant, because of the potential scale, cascading downstream impacts, social disruption, and the increased costs (and waste) associated with replacing existing infrastructure. Alternatively, the response may be to accept a higher level of flooding risk, in which case the costs will be transferred onto those at risk from flooding, including the insurance industry, at least in the short term.

6. Implications of Climate Change for Drought in Australia

If the CSIRO9 simulated changes in climate for enhanced greenhouse conditions were to occur, there would be implications for the incidence and severity of drought. Any decrease in average total rainfall (such as CSIRO9 simulates for parts of southern Australia in winter), and any increase in the frequency of dry spells due to a decline in the number of raindays (as simulated for some regions in Figure 4b), have the potential to increase the frequency and/or severity of droughts and to extend their effects into previously less vulnerable areas. Furthermore, increases in potential evaporation due to higher temperatures could increase drought potential even in regions where total rainfall increases (see Rind *et al.*, 1990). Conversely, the increased frequency of larger rainfall events suggested by Figure 8 may result in reduced drought potential if this results in more substantial soil water recharge between dry spells. Although we can speculate about which of these factors is likely to predominate under different climatic regimes and for different site characteristics, quantification requires detailed modelling of near-surface hydrology.

Assessments of soil water impacts of global warming based on GCM results have been undertaken (e.g. Manabe and Wetherald, 1985, 1987), but it is acknowledged that little confidence can be placed in the results. This is largely due to inadequate representation of near-surface hydrological processes in GCMs (e.g. there is often no representation of vegetation) and the coarse horizontal and vertical resolution at which they operate. This is demonstrated by the comparison of GCM modelled mean soil water content with observations reported for several regions in the former USSR by Vinnikov and Yeserkepova (1991). The three GCMs they studied simulated the phase of the seasonal cycle reasonably well but exaggerated

the amplitude, gave mean conditions considerably in error, and gave unrealistically low values (near zero) not evident in the observations. Rind *et al.* (1990) note that GCMs may significantly underestimate drought intensification because of limitations in the modelling of soil hydrology, particularly the tendency to give unrealistically low soil water. Even without these limitations in the modelling of near-surface hydrological processes, GCM generated hydrology would be of limited value where there are large discrepancies between the observed rainfall and that simulated in the GCM control climate. Furthermore, due to mis-match of scales between rainfall events as simulated in the model and as observed in the real world, daily rainfall frequency distributions must necessarily be poorly simulated in the GCM. This further limits the usefulness of GCM-simulated soil water.

Due to the serious problems associated with GCM-simulated soil water, potential drought impacts are investigated here using a stand alone soil water balance model run off-line from the GCM. Such models have several advantages. They can be set up for specific site characteristics, such as vegetation type and soil hydrologic characteristics. By driving the model with either historical or synthetically generated time series of rainfall and potential evaporation, errors due to a poor rainfall simulation are avoided. To explore the effect of climate change the input time series can be modified in accordance with GCM results. In addition, by using an off-line model, one is not restricted to using a single estimate of future climate (as generated in a particular GCM); a range of plausible future climates can be examined, allowing the sensitivity of the system to be explored. We exploit this opportunity in the current study by using a set of regional climate change scenarios for 2030 based on the results of CSIRO9 and four other recent GCM enhanced greenhouse experiments (Appendix).

The soil water balance model is driven by daily historical time series of rainfall and potential evaporation, the latter derived from Class-A pan evaporation. It is set up for a hypothetical environment of short pasture on a permeable loam soil with an available water capacity (AWC) of 200 mm and no significant water table penetration of the rooting zone. Interception is calculated by an empirical relationship based on those of Feddes *et al.* (1978) and Bultot and Dupreiz (1985). All rainfall is treated as available for soil water recharge, any excess once AWC is filled being treated as run-off. Soil water storage is treated as a single store with evaporation at the potential evaporation rate when the soil water content is above 70% of AWC. For drier conditions, a linear extraction function, as described by Calder *et al.* (1983), is used which reduces evaporation to zero as soil water content approaches wilting point. The water balance model operates iteratively using a daily time step and computes a number of drought related statistics on a seasonal basis. Only results for seasonal soil water deficit (SWD) are presented here.

Detailed results for summer are presented for Perth, Western Australia, to demonstrate the methodology used. Initially, the observed data are used directly, and adjusted by various amounts, to assess the sensitivity of Perth summer SWDs to a range of changes in rainfall and potential evaporation using the response

surface methodology proposed by Fowler and de Freitas (1990). Secondly, potential changes in the frequency of seasonal dryness expected to be exceeded under current climate in one year in five are examined. We then consider potential impacts in terms of the Australian region climate change scenarios, detailed in the Appendix. The analysis is undertaken for nine Australian sites, representing a wide range of rainfall and potential evaporation regimes (Figure 11) and climate change scenarios (Table I). Changes in the number of raindays are not included in the analysis at this stage. This would involve an appropriate modification to the observed rainfall frequency distributions (in line with what is seen in Figure 8) and will form a later step in our research.

The sensitivity of the mean summer SWD in Perth to climate change is shown in Figure 12. Graph axes denote −20% to +40% changes in summer half-year (November–April) rainfall and year-round potential evaporation, applied on a daily basis. The three panels in the figure represent changes in winter half-year rainfall (May–October) of −10%, 0, and +10%, respectively. Isopleths in the body of each graph represent the interacting effect of these changes on mean summer SWD. Current climate (unadjusted input) is represented by the point marked '+' in the centre panel.

Small differences between the three panels in Figure 12 are due to variations in

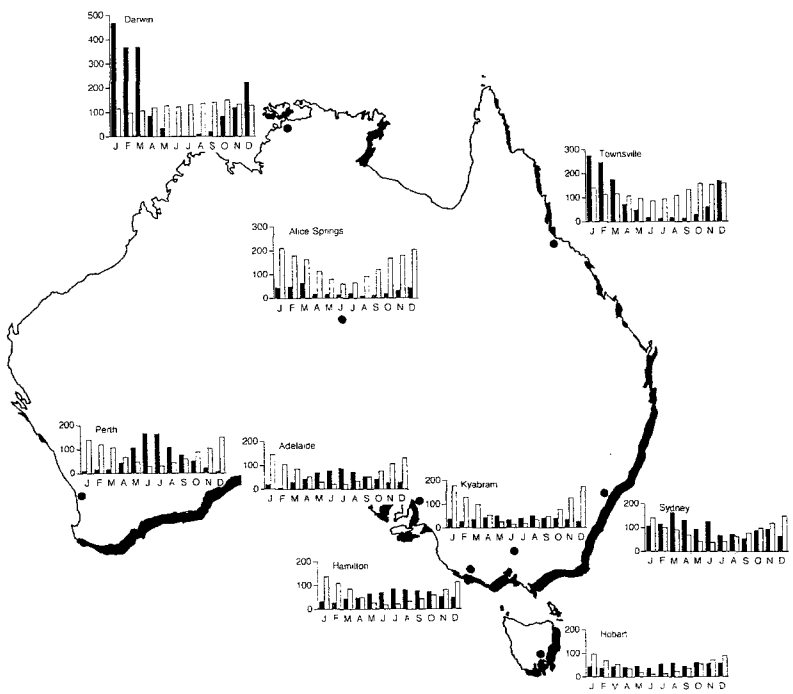

Fig. 11. Locations of the nine sites used in the assessment of potential drought impacts, together with mean monthly precipitation (solid bars) and potential evaporation (open bars) for each site.

TABLE I: Climate change scenarios for the nine sites shown in Figure 11 extracted from the climate change scenarios detailed in the Appendix. Figures are for 2030 and give the range of projected changes in surface air temperature (ΔT), potential evaporation (ΔPE), and rainfall (ΔR) for the summer and winter half-years

Site	ΔT (°C)	ΔPE (%)	ΔR (%)	
			November–April	May–October
Darwin	0–1.5	0–6	0–20	0
Townsville	0–1.5	0–6	0–20	−10—10
Alice Springs	0.5–2.5	1–10	0–20	0
Perth	0.5–2.0	1–8	0–20	−10—10
Adelaide	0.5–2.0	1–8	0–20	−10—0
Hamilton	0.5–2.0	1–8	0–20	−10—10
Kyabram	0.5–2.5	1–10	0–20	−10—10
Sydney	0.5–2.0	1–8	0–20	−10—10
Hobart	0.5–2.0	1–8	0–20	0—10

carried-forward soil water content, in response to changes in winter half-year rainfall. These differences are minor compared to the sensitivity of the soil water regime to changes in summer half-year rainfall and potential evaporation. The shallow slope of the isopleths in Figure 12 indicates greater sensitivity of mean summer SWD to percentage change in potential evaporation than to rainfall. For example, for the central panel in Figure 12, a 40% increase in rainfall reduces the mean summer SWD by 5 mm, whereas a 40% increase in potential evaporation increases it by three times this amount. However, the sensitivity pattern is site specific, reflecting the details of the climate regime (see Figure 11). In general, the

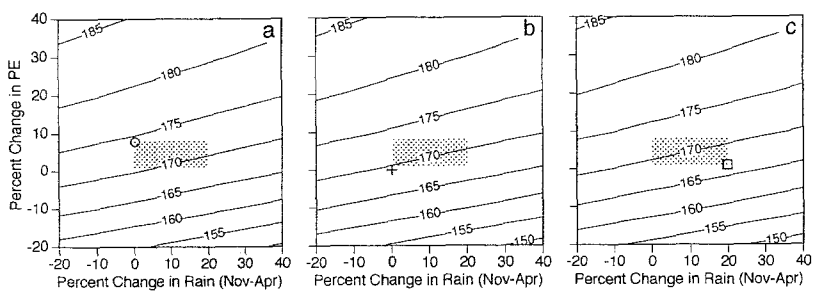

Fig. 12. Response surfaces of the sensitivity of mean summer (DJF) soil water deficit simulated for Perth to change in precipitation and potential evaporation. Panel axes denote −20% to +40% changes in summer half-year (November–April) rainfall and year round potential evaporation. Panels a, b and c represent −10, 0 and +10% changes in winter half-year (May–October) precipitation. Stippling denotes the regional climate change scenario for Perth (see Appendix). The point marked '+' in the centre panel represents current climate. The points marked 'O' and '□' identify the range of potential impacts. The analysis is based on 23 summers from 1967 to 1990. Data source: Australian Bureau of Meteorology.

relative importance of a percentage change in potential evaporation increases with the ratio of summer half-year potential evaporation to rainfall, provided soils are not so dry that increased potential evaporation has little impact. However, isopleth slopes rarely exceed 45 degrees (indicating similar sensitivity to percentage changes in rainfall and potential evaporation) even in very wet summer half-year sites, such as Darwin and Townsville.

Stippled areas superimposed onto the three response surfaces in Figure 12 denote a climate change scenario for Perth at 2030 (Climate Impact Group 1992, Appendix). As Perth is a southern coastal site, projected warming by 2030 is 0.5–2.0 °C which, assuming a 2–4% increase in potential evaporation per degree Celsius, corresponds to a 1–8% increase in potential evaporation by 2030. As for all of Australia, a 0–20% increase in summer half-year rainfall is projected, which is depicted, along with the potential evaporation change, by each of the stippled areas in Figure 12. The projected −10 to +10% change in winter half-year rainfall is represented by the three panels. On the basis of this scenario, plausible mean summer SWDs at Perth by 2030 are in the range 167 mm (marked '□' in Figure 12c) to 174 mm (marked 'O' in Figure 12a), compared to a mean summer SWD of 169 mm under current climate. The scenario envelopes are 'weighted' towards summer drying, but probably the more important result is that the direction of change is uncertain.

An indication of the significance of changes in mean summer SWD of −2 to +5 mm can be gained with reference to current interannual variability. The central (bold) line in Figure 13 gives the probability of a given summer mean SWD being exceeded, based on simulation results for 23 summers. A summer mean SWD of 169 mm under current climate is exceeded in approximately 62% of summers, compared to 65% for 167 mm and 31% for 174 mm. The potential reduction in drying is clearly small, whereas the potential increase is quite substantial, involving a shift to new mean conditions which are currently only experienced about once in three years.

To assess potential changes in the frequency of relatively dry summers, revised exceedance probability curves were derived for the two points on the scenario overlays representing the range of plausible impacts (i.e. the point of maximum drying marked 'O' in Figure 12a, and the point denoting the largest reduction in drying marked '□' in Figure 12c). The resulting exceedance probability curves straddle the curve for current climate in Figure 13. The area between the curves can be viewed as a potential impacts envelope.

The exceedance probability curves in Figure 13 can be used to assess potential changes in the magnitude of summer dryness corresponding to a given probability of occurrence, or the change in the frequency of occurrence of selected levels of soil dryness. For example, under current climate, the 5-year summer soil dryness 'event' (20% exceedance probability) is 179 mm. According to the climate change scenario, the summer mean SWD with the same return period would be between 178 and 182 mm by 2030. Alternatively, and probably more usefully, the current five year event might occur 10% less or up to 75% more frequently.

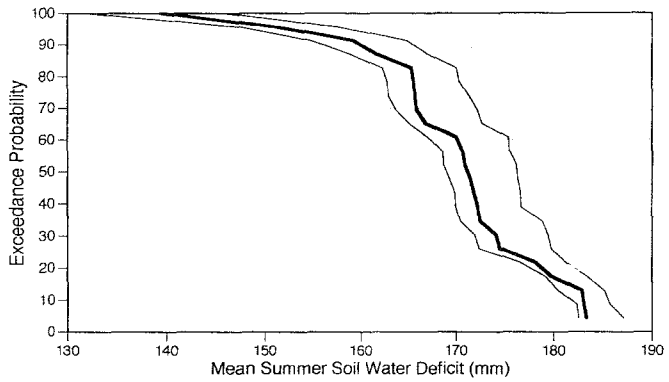

Fig. 13. Summer mean soil water deficit exceedance probability curves for Perth. The central bold curve gives the probability of a summer mean soil water deficit being exceeded under current climate, based on results from 23 summers of simulated soil water deficit data. Curves above and below this line are for identical analyses for the two points marked 'O' and '□' in Figure 12. The upper line, (maximum drying and marked 'O' in Figure 12a), was derived by running the water balance model with no change in summer half-year rainfall, winter half-year adusted by −10%, and potential evaporation by +8%. The lower line (maximum reduction in soil dryness and marked '□' in Figure 12c) was derived by running the water balance model with summer half-year rainfall increased by +20%, winter half-year rainfall by +10%, and potential evaporation by +1%.

The analysis outlined above was repeated for all seasons at eight additional sites around Australia, representing a wide range of climate regimes and several different climate change scenarios. The nine sites used are shown in Figure 11 together with mean monthly rainfall and potential evaporation. Potential impacts are presented in Figure 14 in terms of percentage change in the frequency of the simulated seasonal mean SWD with a 20% chance of occurrence under current climate.

Results for summer (DJF) in Figure 14 indicate relatively small potential impacts on the soil water regime with changes within the bounds +100% and −50% at all sites. Maximum drying is simulated for the two 'Mediterranean-type' climates (Perth, Adelaide), characterised by dry, warm to hot summers and mild winters. Potential impacts in autumn (MAM) are dominated by decreases in soil dryness, especially in the southeast and southwest of the country. Some potential drying is simulated at all sites but this is minor in all cases. Results for winter (JJA) indicate the greatest potential for increased soil drying (in terms of the number of sites significantly affected) with the frequency of the current 5-year event more than doubling at four of the nine sites. Three sites indicate potential significant decreases (Perth, Adelaide, Hamilton) with almost a halving of the frequency of the current 5-year event. Two of these (Perth, Hamilton) are amongst the four sites indicating possible significant drying. Potential impacts in spring (SON) are the most extreme of any season. Greater than 100% increases in the frequency of the 5-year event are simulated for the two Mediterrannean-type climates (Perth, Adelaide) while up to a 75% reduction is simulated for Hobart. It must be noted that changes of a given percentage in Figure 14 may differ very much from site to site and season to season

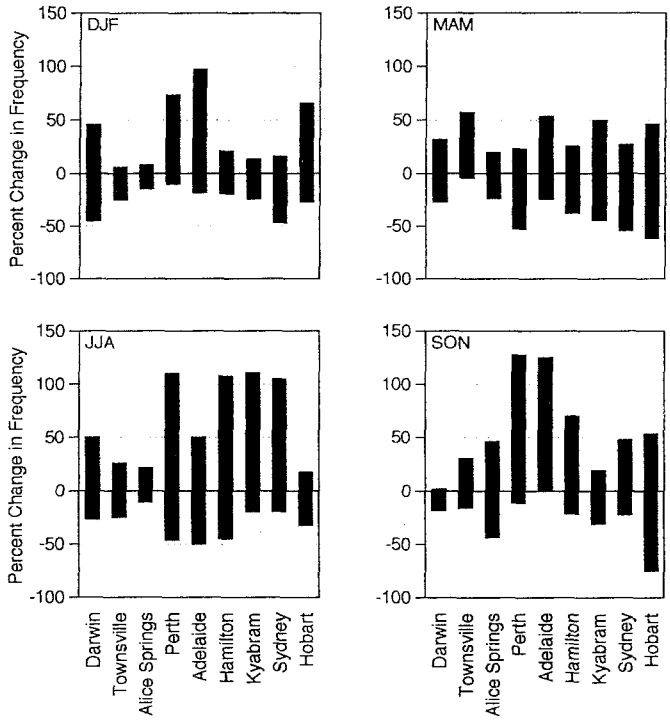

Fig. 14. Percentage change in the frequency of occurrence of the simulated mean seasonal soil dryness exceeded on average once in five years under current climate. Results are derived from analysis of potential impacts envelopes (e.g. Figure 13) representing the range of impacts consistent with the regional climate change scenario. The nine sites shown represent a range of climate regimes (Figure 11) and climate change scenarios (see Appendix).

in terms of their practical significance. For example, marked changes in the return period of the current 5-year dry event in seasonally very dry sites (such as Perth in summer) may not be as important as similar changes at seasonally moderately wet sites (such as the southeast Australian sites in spring).

Significant SWD impacts are largely confined to the south of Australia, with relatively little potential for either increased or decreased soil dryness simulated for the three northern sites (Darwin, Townsville, Alice Springs). Potential increases in dryness are greatest for the Mediterranean-type climates of Perth and Adelaide. Differentiating the results on the basis of the climate change scenario is difficult due to the small number of sites, but results do broadly follow intuitive expectations based on the characteristics of the scenario. For example, potential impacts show a greater range in winter half-year rainfall sub-region B (see Appendix), due to uncertainty about the direction of change of winter half-year rainfall. Similarly, the large difference in potential change in soil dryness in spring between Adelaide and Hobart partly reflects the fact that, in accordance with the scenario, winter half-year rainfall is permitted to increase at Hobart but not at Adelaide. Changes in

potential impacts associated with variation in the increase in temperature are largely obscured by differences associated with climate regime and rainfall change.

Although some of the patterns described above are noteworthy, probably the single most important feature of Figure 14 is the fact that, with the exception of Adelaide in spring, assessment of potential impacts indicates that the direction of soil-water regime change is uncertain across all sites and seasons. Therefore, we remain unable to make even guarded statements about whether climate change in the Australian region can be expected to lead to increased or decreased drought potential. At best, we can suggest the more likely direction of change (for some seasons and localities) and give some indication of the potential scale of that change. However, even such a general statement must be heavily qualified. The results cited above are dependent on the climate change scenarios used which contain significant sources of uncertainty. Note that this uncertainty includes that associated with the sensitivity of global climate due to increased greenhouse gas concentrations and that associated with projections of future greenhouse gas emissions (see Appendix). It does not include that associated with possible changes in the frequency and magnitude of ENSO. Were ENSO to change its nature due to global warming, the effects of this would have to be considered in addition to those changes which have been explored here. Additional uncertainty is added by the fact that the scenario does not account for possible cooling associated with sulfate aerosols, possible negative feedback due to CO_2 fertilisation (Wigley and Raper, 1992), nor for possible reductions in transpiration resulting from stomatal response to increased atmospheric CO_2.

7. Conclusions

Any conclusions drawn from this study must take into account the significant caveats outlined in Section 2. The limitations of greatest significance are: the crude nature of rainfall simulation in current GCMs; the related problem of the mismatch in spatial scales between GCM-simulated grid point rainfall and rainfall events as they are observed in the real world; and the inability to incorporate possible changes in ENSO into the current study.

Taking into account the caveats, a number of significant conclusions can still be drawn from this study. Modelling results, supported by theory, indicate that the frequency distribution of daily rainfall may change significantly due to the enhanced greenhouse effect. In particular, for the Australian region, the CSIRO9 model shows a marked increase in the frequency of heavy rainfall days. This signal is stronger and more coherent in the Australian region than changes in total rainfall. Similar results have been obtained with other models. The most important manifestation of these changes, if they were to occur, would be an increase in the frequency of extreme rainfall events and associated flooding. The caveats are such that we cannot, on the basis of this study, say how large any such increase in frequency may be. However, because of the potential significance of such changes, and their

magnitude at the grid-box scale in the GCM, the subject deserves a high priority in further research.

Our scenario-based assessment of potential impacts of climate change on seasonal soil water deficits over Australia suggests that drought potential may not change significantly in the North of the region characterised by summer half-year rainfall. Potential changes are largest in the south of the country, with Mediterranean-type climates apparently most liable to increased drought potential. The south of Australia is also characterised by the greatest uncertainty, largely due to the fact that four of the sites lie in a region for which the scenarios give an uncertain direction of change in winter half-year rainfall. However, perhaps the most important result emerging from the analysis is the fact that even the direction of change is at present uncertain at all sites and for all seasons (Adelaide in spring is the one exception). It should be noted that the results presented here do not take into account possible changes in the frequency of rainy days, and are specific to a single set of site characteristics. Potential impacts will differ, possibly significantly, for different vegetation types and soil characteristics. However, it is clear that substantial further research is required before we can expect to say anything definitive about the impact of climate change on drought in the Australian region.

Appendix: Australian Region Climate Change Scenarios

The full details of this set of climate change scenarios are given in Climate Impact Group (1992). In this appendix we describe only those parts of that set of scenarios required for application in the soil water analysis of Section 5. These are the ranges of change in rainfall, temperature and evaporation for 2030. Note that these scenarios have the shortcoming of the GCMs upon which they are based (see discussion in Section 2).

We use here the results of enhanced greenhouse GCM experiments conducted with: CSIRO9, the Bureau of Meteorology Research Centre model (BMRC) (McAvaney *et al.*, in press); and the three high resolution experiments used in Houghton *et al.* (1990) namely: the United Kingdom Meteorological Office high resolution model (UKMOH), the Geophysical Fluid Dynamics Laboratory high resolution model (GFDLH), and the Canadian Climate Centre model (CCC). All these experiments used a simple mixed layer ocean without ocean currents, but with a heat flux correction. The experiments were run to equilibrium for $1 \times CO_2$ and $2 \times CO_2$ conditions. In our assessment the main broadscale climatic features of the Australian region were simulated by each model under current conditions, and we concluded that the $2 \times CO_2$ results of all five experiments should be given equal weight in assessing possible regional climate change.

The results were used to prepare scenarios of the spatial pattern of temperature and rainfall change in the Australian region. To obtain these, the $2 \times CO_2$ results were re-expressed as the pattern of temperature change, or percentage rainfall change, per degree of global warming. For each grid point (on an interpolated common grid) the simulated changes were then ranked from the highest to the lowest. Seasonal maps of the rank 2 and rank 4 changes (the 80th and 20th percentiles) were then examined. These maps were taken to represent the range of regional temperature and rainfall change per degree of global warming indicated by the five models. For temperature the ratio of local warming to global warming was around 0.3–1.0 in northern coastal areas of Australia; a little greater in southern coastal areas (0.8–1.2); and encompassed a large range in inland Australia (0.5–1.4).

Scenarios of climate change in the Australian region for particular times in the future can then be constructed by multiplying the regional response estimates by estimates of global warming. For this purpose, we have used the recent transient global warming scenarios of Wigley and Raper (1992) which take into account uncertainty in the sensitivity of global climate to greenhouse gas forcing (global equilibrium warming of 1.5–4.5 °C for a doubling of CO_2, see Houghton *et al.*, 1990) and

TABLE II: Estimates of the range of temperature change for locations in the Australian region. 2030 values are rounded to the nearest half degree

Region	Local warming per degree global warming (°C)	Warming in 2030 (°C)
Northern Coast (north of about 25° S)	0.3–1.0	0–1.5
Southern Coast (south of about 25° S)	0.8–1.2	0.5–2.0
Inland (more than about 200 km from coast)	0.5–1.4	0.5–2.5

uncertainty in future emissions of greenhouse gases. The curves we took from Wigley and Raper (1992) were those that did not take into account the possible effect of sulfate aerosol or CO_2 fertilisation, as we felt that these factors were yet to be sufficiently well quantified. Table II gives warming scenarios for Australia scaled in this way for 2030.

Scenarios of changes in potential evaporation are constructed as needed from the temperature scenarios assuming an increase of 2–4% in potential evaporation per degree of regional warming. The range represents uncertainty in this relationship. Shuttleworth (1983) suggests a figure of 2% increase in potential evaporation per °C while Budyko (1980, cited in Nemec and Schaake, 1982) gives an average relation of 4% per °C. Rosenberg *et al.* (1990) derive values in excess of 6% per °C for changes in temperature alone, but lower values when potential feedbacks, such as increased humidity in the lower atmosphere, are accounted for.

Figure 15 shows the regional distribution of the number of models showing an increase in rainfall for the summer and winter half years. In summer, at least four of the five models indicate rainfall increases across nearly all of Australia, and in many regions all five show increases. In winter, all models show increases south of around 40° S, and at least four of the five models show decreases over inland southern areas of Australia. Between these zones (southern and south-eastern coastal Australia) the models disagree on the sign of the rainfall change.

Based on the spatial patterns presented in the figure and the 20 and 80 percentile maps for rainfall changes, the simulated response of Australian rainfall per degree of global warming can be characterised as follows: in the summer half-year increases of 0–10% for locations throughout the continent; in the winter half-year decreases of 0–5% in southern inland areas, increases or decreases of 0–5% in southern and southeastern coastal areas and increases of 0–5% for regions south of 40° S. The resulting scenarios, scaled as for temperature for 2030, are given in Table III, and the three regions used in this table for the winter half year rainfall scenario are given in Figure 16.

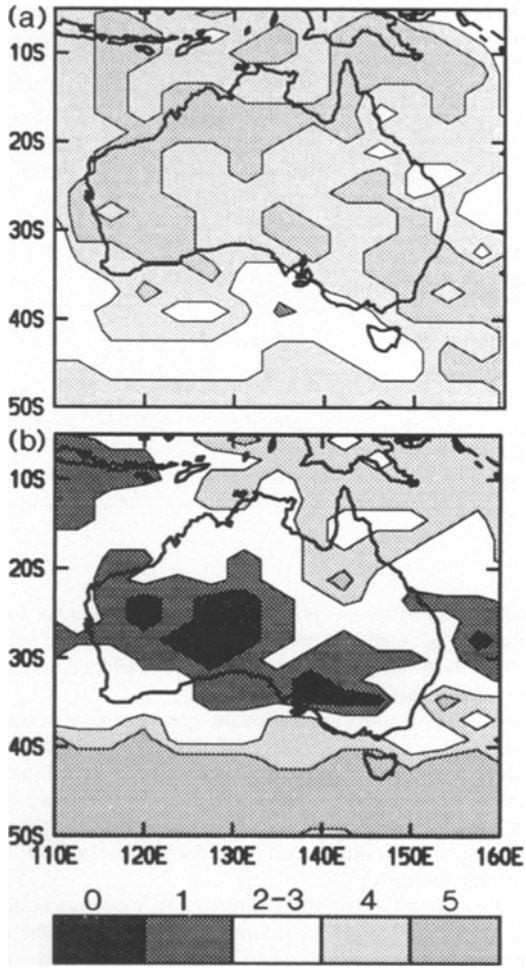

Fig. 15. Number of GCMs (maximum of five) showing an increase in rainfall under enhanced greenhouse conditions: (a) summer half-year (Nov.–Apr.); (b) winter half-year (May–Oct.).

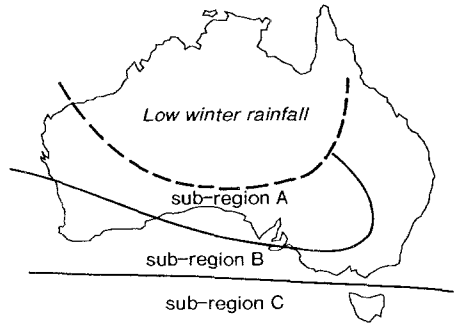

Fig. 16. Subregions used for winter rainfall change (see Table III).

TABLE III: Scenarios of rainfall change for locations in the Australian region for 2030. Subregions are as defined in Figure 16. 2030 values are rounded to the nearest 10%

Season	Region	Response per degree global warming	Change in 2030
Summer half-year (Nov. to April)	Any location	0–+10%	0–+20%
Winter half-year (May to Oct.)	Locations in subregion A	0–−5%	0–−10%
	Locations in subregion B	−5–+5%	−10–+10%
	Locations in subregion C	0–+5%	0–+10%

Acknowledgements

The GCM data used here was generously provided by climate modellers at CSIRO, Bureau of Meteorology Research Centre, Geophysical Fluid Dynamics Laboratory, United Kingdom Meteorological Office and the Canadian Climate Centre. We thank M. Hulme of University of East Anglia for providing details of the data presented in Wigley and Raper (1992). The program used for assessing field significance was kindly supplied to us by K. Walsh of CSIRO. This work was supported by funds provided as part of climate change research agreements with the Governments of New South Wales, Victoria, Western Australia, the Northern Territory and the Commonwealth Department of the Arts, Sport, the Environment and Territories.

References

Budyko, M. I.: 1980, 'Klimat v Proslom Budustem (Climate in the Past and in the Future)', Mysi Publishers, Moscow, (in Russian).

Bultot, F. and Dupriez, G. L.: 1985, 'Daily Effective Evapotranspiration from a River Basin', *Casebook on Operational Assessment of Areal Evaporation*, Operational Hydrology Rpt. No. 22, WMO, Geneva, 80–103.

Calder, I. R., Harding, R. J., and Rosier, P. T. W.: 1983, 'An Objective Assessment of Soil Moisture Deficit Models', *J. Hydrol.* **60**, 329–355.

Campbell, R., Crowley, P., and Demura, P.: 1983, 'Impact of Drought on National Income and Employment', *Quart. Rev. Rural Econ.* **5**, 254–257.

Climate Impact Group: 1992, 'Climate Change Scenarios for the Australian Region', Available from CSIRO Division of Atmospheric Research, Aspendale, Australia.

Feddes, R. A., Kowalik, P. J., and Zaradny, H.: 1978, 'Simulation of Field Water Use and Crop Yield', *Simulation Monographs*, Centre for Agricultural Publishing and Documentation, Wageningen.

Fowler, A. M. and de Freitas, C. R.: 1990, 'Climate Impact Studies from Scenarios: Help or Hindrance?', *Weath. Clim.* **10**, 3–9.

Gordon, H. B., Whetton, P. H., Pittock, A. B., Fowler, A. M., and Haylock, M. R.: 1992, 'Simulated

Changes in Daily Rainfall Intensity Due to the Enhanced Greenhouse Effect: Implications for Extreme Rainfall Events', *Clim. Dynam.* **8**, 83–102.

Hansen, J., Rind, D., DelGenio, A., Lacis, A., Lebedeff, S., Prather, M., Ruedy, R.: 1988, 'Regional Greenhouse Climate Effects', in *Coping with Climate Change*, Proc. Second N. Amer. Conf. on Preparing for Clim. Change, Dec. 6–8, (Climate Institute, Wash. DC, 1989), 68–81.

Hennessy, K. J., Fowler, A. M., and Whetton, P. H.: 1993, 'GCM Simulated Changes in Daily Rainfall Intensity and Heavy Rainfall Events under an Enhanced Greenhouse Effect', Preprints, Fourth International Conference on Southern Hemisphere Meteorology and Oceanography, Hobart March 1993, AMS, 199–200.

Houghton, J. T., Jenkins, G. J., and Ephraums, J. J. (eds.): 1990, *Climate Change, The IPCC Scientific Assessment*, Cambridge University Press, Cambridge, 365 pp.

Houghton, J. T., Callander, B. A., and Varney, S. K. (eds.): 1992, *Climate Change 1992: The Supplementary Report to the IPCC Scientific Assessment*, Working Group 1, Bracknell, Cambridge University Press, Cambridge.

Jaeger, L.: 1976, 'Monatskarten des Niederschlags für die Ganze Erde', *Bericht Deutsch. Wetterd.* **18** (139).

Joy, C. S.: 1991, 'The Cost of Natural Disasters in Australia', paper presented at the workshop 'Climate Change Impacts and Adaptation: Severe Weather Events', Climate Impacts Centre, Macquarie University, NSW, Australia 13–15 May, 9 pp.

Lynch, A. H.: 1987, 'Australian East Coast Cyclones III: Case Study of the Storm of August 1986', *Austral. Meteorol. Magaz.* **35**, 163–170.

McAvaney, B. J., Colman, R. A., Fraser, J. R., and Dahni, R. R.: in press, 'The Seasonal Climatic Response to a Doubling of CO_2 as Simulated by the BMRC Atmospheric GCM/Mixed Layer Ocean Model', *Geophys. Res. Lett.*

McGregor, J. L., Gordon, H. B., Watterson, I. G., and Dix, M. R.: 1993, 'The CSIRO 9-Level Atmospheric General Circulation Model', *CSIRO Div. Atmos. Res. Tech. Pap. No. 26.*, CSIRO Australia, 89 pp.

Manabe, S. and Wetherald, R.: 1985, 'CO_2 and Hydrology', *Advances Geophys.* **28A**, 131–157.

Manabe, S. and Wetherald, R.: 1987, 'Large-Scale Changes of Soil Wetness Induced by an Increase in Atmospheric Carbon Dioxide', *J. Atmos. Sci.* **44**, 1211–1236.

Mearns, L. O., Schneider, S. H., Thompson, S. L., and McDaniel, L. R.: 1990, 'Analysis of Climate Variability in General Circulation Models: Comparison with Observations and Changes in Variability in $2 \times CO_2$', *J. Geophys. Res.* **95**, 20469–20490.

Meehl, G. A., Branstator, G. W., and Washington, W. M.: 1993, 'Tropical Pacific Interannual Variability and CO_2 Climate Change', *J. Clim.* **6**, 42–63.

Nemec, J. and Schaake, J.: 1982, 'Sensitivity of Water Resources Systems to Climate Variation', *Hydrol. Sci. J.* **27**, 327–343.

Nicholls, N. and Woodcock, F.: 1981, 'Verification of an Empirical Long-Range Weather Forecasting Technique', *Quart. J. Roy. Meteorol. Soc.* **107**, 973–976.

Noda, A. and Tokioka, T.: 1989, 'The Effect of Doubling the CO_2 Concentration on Convective and Non-Convective Precipitation in a General Circulation Model Coupled with a Simple Mixed Layer Ocean Model', *J. Meteorol. Soc. Japan* **67**, 1057–1069.

Pittock, A. B.: 1975, 'Climatic Change and Patterns of Variation in Australian Rainfall', *Search* **6**, 498–504.

Pittock, A. B.: 1984, 'On the Reality, Stability, and Usefulness of Southern Hemisphere Teleconnections', *Austral. Meteorol. Magaz.* **32**, 75–82.

Pittock, A. B.: in press, 'A Climate Change Perspective on Grasslands', Proc. XVII Int. Grasslands Congress, February 1993, Massey University, Palmerston North, NZ.

Preisendorfer, R. W. and Barnett, T. P.: 1983, 'Numerical Model-Reality Intercomparison Tests Using Small Sample Statistics', *J. Atmos. Sci.* **40**, 1884–1896.

Rind, D., Goldberg, R., and Ruedy, R.: 1989, 'Change in Climate Variability in the 21st Century', *Clim. Change* **14**, 5–37.

Rind, D., Goldberg, R., Hansen, J., Rosenzweig, C., and Ruedy, R.: 1990, 'Potential Evapotranspiration and the Likelihood of Future Drought', *J. Geophys. Res.* **95**, 9983–10004.

Robinson, D. K.: 1987, 'Selection of Design Floods', in Pilgrim, D. H. (ed.), *Australian Rainfall and*

Runoff: A Guide to Flood Estimation, Vol. 1, The Institute of Engineers, Australia, Barton, ACT, Australia.

Rosenberg, N. J., Bruce, A., Kimball, P. M., and Cooper, C. F.: 1990, 'From Climate and CO_2 Enrichment to Evapotranspiration', in Waggoner, P. E. (ed.), *Climate Change and U.S. Water Resources*, Wiley, New York, pp. 151–175.

Shuttleworth, W. J.: 1983, 'Evaporation Models in the Global Water Budget', in Street-Perrott, A., Beran, M., and Ratcliffe, R. (eds.), *Variations in the Global Water Budget*, Reidel, Dordrecht, pp. 147–171.

Smith, D. I. and Greenaway, M. A.: 1987, *Dam Failure, The Estimation of Direct Flood Damage, a Study of Queanbeyan, NSW*, Working paper 1987/23, Centre for Resource and Environmental Studies, ANU, Canberra, 53 pp.

Stephens, G. L.: 1990, 'On the Relationship between Water Vapour over the Oceans and Sea Surface Temperature', *J. Clim.* **3**, 634–645.

Vinnikov, K. Ya. and Yeserkepova, I. B.: 1991, 'Soil Moisture: Empirical Data and Model Results', *J. Clim.* **4**, 66–79.

Wetherald, R. T. and Manabe, S.: 1988, 'Cloud Feedback Processes in a General Circulation Model', *J. Atmos. Sci.* **45**, 1397–1415.

Whetton, P. H.: 1993, 'Assessing Possible Climate Change in the Australian Region', Preprints, Fourth International Conference on Southern Hemisphere Meteorology and Oceanography, Hobart March 1993, AMS, 355–356.

Whetton, P. H. and Pittock, A. B.: 1991, *Australian Region Intercomparison of the Results of Some General Circulation Models Used in Enhanced Greenhouse Experiments*, CSIRO Division of Atmospheric Research Technical Paper No. 21, 73 pp.

Wigley, T. M. L. and Raper S. C. B.: 1992, 'Implications for Climate and Sea Level of Revised IPCC Emissions Scenarios', *Nature* **357**, 293–300.

Wigley, T. M. L. and Santer, B. D.: 1990, 'Statistical Comparison of the Spatial Fields in Model Validation, Perturbation, and Predictability Experiments', *J. Geophys. Res.* **95**, 851–856.

Wilson, C. A. and Mitchell, J. F. B.: 1987, 'Simulated CO_2 Induced Climate Change over Western Europe', *Clim. Change* **10**, 11–42.

WMO: 1992, *Simulation of Interannual and Intraseasonal Monsoon Variability*, Report WCRP-68, WMO/TD-No. 470, World Climate Research Program, World Meteorological Organisation, Geneva.

(Received 26 June, 1992; in revised form 26 July, 1993)